Geoderma 429 (2023) 116255

Contents lists available at ScienceDirect

Geoderma

journal homepage: www.elsevier.com/locate/geoderma

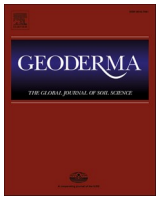

Differential bacterial ammonia oxidation patterns in soil particles from two contrasting forests: The importance of interfacial interactions

Xiaohu Wang [a,b], Xiaoming Wang [c], Wantong Zhao [c], Ran Yu [d], Junkang Wu [e], Yongping Kou [a], Qing Liu [a], Wenqiang Zhao [a,*]

[a] CAS Key Laboratory of Mountain Ecological Restoration and Bioresource Utilization & Ecological Restoration Biodiversity Conservation Key Laboratory of Sichuan Province, Chengdu Institute of Biology, Chinese Academy of Sciences, Chengdu 610041, China
[b] University of Chinese Academy of Sciences, Beijing 100049, China
[c] Key Laboratory of Arable Land Conservation (Middle and Lower Reaches of Yangtze River), Ministry of Agriculture and Rural Affairs, College of Resources and Environment, Huazhong Agricultural University, Wuhan 430070, China
[d] Department of Environmental Science and Engineering, School of Energy and Environment, Southeast University, Nanjing 210096, China
[e] Department of Water Supply and Drainage, Nanjing Forestry University, Nanjing 210037, China

ARTICLE INFO

Handling Editor: Naoise Nunan

Keywords:
Subalpine forest
Soil particle
Ammonia-oxidizing bacteria
Interfacial interaction
Nitrogen availability
Metabolic activity

ABSTRACT

Soil inorganic nitrogen (N) deficiency limits forest productivity in subalpine regions. The traditional view holds that subalpine coniferous forests are characterized by lower soil inorganic N availability, and such differences are greatly affected by the diversity and abundance of ammonia-oxidizing bacteria. It is known that interfacial interactions between bacteria and solid particles in agricultural and aquatic ecosystems can alter bacterial metabolic activity and biogeochemical processes. However, whether bacteria-soil interfacial interactions induce different ammonia oxidation processes in distinct soil particles remain unknown. Herein, we collected soil particles of different sizes from two contrasting forest sites (a spruce-dominated natural forest and spruce plantation) and examined the effect of soil-*Nitrosomonas europaea* (a model ammonia-oxidizing bacteria) interfacial interactions on the oxidation of ammonium (NH_4^+-N) using batch adsorption and semipermeable membrane experiments. The metabolic activity of bacteria was also examined using an isothermal microcalorimetric method. Upon adsorption on soil particles, the ammonia oxidation rate and bacterial metabolism activity were slower than those of free bacteria. The inhibition effect ceased when the bacteria were physically isolated from the soil particles by a membrane, indicating the importance of interfacial interactions in the ammonia oxidation process. Additionally, clay particles were more effective than silts and sands in binding cells and greatly reduced the ammonia oxidation reaction. Across the two forests, natural forest soils exhibited a higher bacterial adsorption capacity but lower bacterial metabolic activity, resulting in a fewer loss of NH_4^+-N. Our results suggested that stronger bacteria-soil interfacial interactions (especially for clay fractions) were responsible for maintaining high soil inorganic N availability in forests, highlighting the need to incorporate interfacial interactions into biogeochemical models of N cycling in forest ecosystems.

1. Introduction

Microorganisms can be transported with flowing liquid or retained by solid surfaces (Ahmed and Holmström, 2015; He et al., 2021). Substantial research efforts have revealed the massive potential of microbe-solid surface interfacial interactions for regulating a broader range of biogeochemical processes (Pronk et al., 2016; Zhu et al., 2022). Reactions occurring at interfaces are involved in microbial community variation, cell metabolic function, nutrient cycling, fate of polluting elements, and organic matter transformation dynamics (Putnis and Ruiz-Agudo, 2013; Putnis, 2014; Pronk et al., 2016; Wang and Putnis, 2020; Kleber et al., 2021). The magnitudes of interfacial interactions largely depend on solid types (e.g., metal oxide, silicates, clay mineral, and soil particle), particle size distribution, surface physico-chemical properties (e.g., specific surface area, pore size, pore volume, surface functional groups, zeta potential and hydrophobicity) and solution composition (e.g., pH, ion type and ionic strength) (Gupta and Sen, 2017; Kleber et al., 2021). Mechanisms of interfacial interactions can be

* Corresponding author at: Chengdu Institute of Biology, Chinese Academy of Sciences, P.O. Box 416, Chengdu 610041, China.
E-mail address: zhaowq@cib.ac.cn (W. Zhao).

https://doi.org/10.1016/j.geoderma.2022.116255
Received 15 May 2022; Received in revised form 31 October 2022; Accepted 5 November 2022
Available online 12 November 2022

explained by electrostatic adsorption, surface complexation, ion exchange, and precipitation (Putnis and Ruiz-Agudo, 2013; Nell and Fein, 2017; Chen et al., 2019; Zhu et al., 2022). To date, few studies have revealed the interfacial mechanisms governing nutrient transformation in soil particles from different ecosystems. Explicit investigations on how soil particle fractions with varied surface properties trigger interfacial interactions are essential to understand microbe-mediated nutrient cycling in terrestrial ecosystems.

Researchers have attempted to decipher interfacial interaction from both experimental and modeling perspectives to evaluate its potential impacts on environmental and human health. Historically, previous studies mainly focused on the interfacial interactions between solids and bacteria, especially for manure-borne zoonotic pathogens (i.e., *Escherichia coli O157:H7)* (Cai et al., 2018), pesticide degrading bacteria (i.e., *Pseudomonas* spp) (Biswas et al., 2015), metal-reducing bacteria (i.e., *Shewanella oneidensis*) (Mohamed et al., 2020), and plant growth-promoting bacteria (i.e., *Raoultella planticola*) (Li et al., 2021). Bacteria are capable of utilizing soil particles-sorbed contaminants and nutrients, and these interfacial interactions are frequently found in terrestrial environments (Kleber et al., 2021; Aftabtalab et al., 2022). For example, the sorption of *Pseudomonas* sp. Z1 onto montmorillonite enhanced methyl parathion (MP) biodegradation, indicating the importance of bacteria-MP-mineral interfacial interactions in the biodegradation of contaminants in soil systems (Rong et al., 2019). In addition, the clay mineral-microorganism complex interfacial reactions controlled the speciation, mobility and bioavailability of heavy metals in soils and sediments systems (Martinez et al., 2016; Qu et al., 2019). Previous literature has also demonstrated that the chromium (VI) bioreduction kinetics was enhanced when they interacted with iron minerals and *Shewanella oneidensis* (Mohamed et al., 2020). Indeed, environmental nutrient ions (e.g., ammonium (NH_4^+), nitrate (NO_3^-), and phosphate (PO_4^{3-})) almost inevitably come into contact with the surface of solids, and this interfacial interaction can influence nutrient transformation processes (Kleber et al., 2021; Lu et al., 2022). For example, both *Pseudomonas fluorescens* and *Bacillus subtilis* could inhibit P sorption on the soil colloid, which was attributed to increasing soil negative charges by bacteria and chemical interactions of bacteria with soil colloids (Malham et al., 2014; Hong et al., 2021). Another study has showed that high concentrations of suspended sediment promoted the removal of N by ammonium-oxidizing bacteria (AOB) from river water (Xia et al., 2009). However, most research on the interfacial interactions of nutrients primarily focused on environmental pollution rather than plant growth. Therefore, it has become increasingly important to understand the fate of bacteria in soils, which will help to mitigate the risk of nutrient scarcity, microbial pathogens contamination, and food resources. Actually, plants face harsh conditions in which nutrients may be depleted, and they mainly absorb and utilize inorganic nutrients in soil solutions. The transformation of plant-unavailable nutrients to plant-available nutrients requires nutrient-transformation-related bacteria (Fraser et al., 2015; Liu et al., 2018). Although there is emerging consensus regarding the fundamental role of adsorbed-state nutrients in ecosystem functions (Plaimart et al., 2021), the effects of bacteria-soil interfacial interactions on soil nutrient availability and subsequent plant performance remain unclear.

Microbial metabolic activities can be greatly impacted by interfacial interactions (Elbourne et al., 2019). Some studies found that the interfacial interactions suppress bacterial metabolic activities (Asadishad et al., 2013). For example, both goethite and the humic acid (HA)-goethite complex depressed *Pseudomonas* sp. Z1 activity and MP degradation (Zhao et al., 2018). Solid-bacteria interactions may decrease microbial metabolic activity by suppressing nutrient acquisition (Zhao et al., 2012), interfering with respiration (Lyon et al., 2008), releasing toxic metal cations (Gold et al., 2018) or damaging membrane integrity (Combarros et al., 2016). In contrast, interfacial interactions can also increase the activity of microbes by enhancing aeration or reducing the exposure of microorganisms to pollutants (Wu et al., 2019), which promote the persistence of microbes in the environment. For instance, the combination of high relative humidity and hygroscopic clay surface stimulated the metabolic activity of microbial communities (Stone et al., 2016). Overall, the interfacial interactions can either stimulate or inhibit bacterial metabolic activities by influencing bioavailable substrates, oxygen levels, and secondary metabolism (Zobell, 1943; Li et al., 2020). Experimental evidence for interfacial interaction effects on the metabolic activity of plant growth-associated bacteria is lacking. Based on the investigations presented above, we inferred that the interfacial interactions between bacteria and soil particles can greatly regulate nutrient-transforming bacterial metabolic activity and thus nutrient availability.

Soils exhibit a complex hierarchical structure with different-sized fractions. The various soil particle size fractions provide spatially heterogeneous conditions for bacteria (Zhang et al., 2017). Physico-chemical properties have been proposed to govern solid particle-bacteria interfacial interactions and bacterial activities (Uroz et al., 2015). Many studies reported that strong physical force induced tight adhesion of bacterial cells on the surface of small particles (Cuadros, 2017; Liu et al., 2017). Clay, owing to its high specific surface area and specific surface electrical properties, provides favourable conditions for bacteria by buffering suspension pH or adsorbing toxic metabolites for optimal growth (Small et al., 1994; Cai et al., 2018). Recent investigation in a long-term fertilizer experiment also revealed that particle-size fractions had strong effects on the abundance of ammonia-oxidizing microorganisms (AOM), and potential nitrite oxidation activity was lower in the silt fraction and higher in the clay fraction, which was closely correlated with the soil total N (TN) (Han et al., 2020; Han et al., 2021). However, the effects of heterogeneous soil particles on bacterial activity and N availability in soils are still unclear. Taken together, the soil particles with various surface physio-chemical properties are important factors in determining bacterial activities and subsequent nutrient transformation.

Thus, the objective of this study was to investigate whether interface interactions could generate divergent bacterial ammonia oxidation patterns in different soil particles. Two alpine coniferous forest sites (i.e., a natural forest and a spruce plantation) with five soil particle sizes (particles with diameters of < 2 μm, 2–53 μm, 53–250 μm, 250–2000 μm, and 0–2000 μm) were selected as model to test the following hypothesis. *Nitrosomonas europaea* (*N. europaea*) strain ATCC 19718 is a ubiquitous participant in the conversion of N in the soil environment and is widely prevalent in acidic forest soils (Carnol et al., 2002). The influences of different soil particles on the bacterial oxidation of NH_4^+-N were investigated by adsorption, oxidation, semipermeable membrane and microcalorimetric experiments. We hypothesized that (i) different soil particles with specific surface physico-chemical properties would differentially impact the strength of interfacial interactions, (ii) bacteria-clay interfacial interactions induce a stronger protection of NH_4^+-N than silts and sands, (iii) the interfacial interactions between soil fractions and AOM reduce AOM metabolic activity and lower NH_4^+-N oxidation rate, and these reactions will result in a higher NH_4^+-N availability.

2. Materials and methods

2.1. Site description

Soil samples were collected from two contrasting sites located approximately 300 m apart in the Miyaluo Experimental Forest in Lixian County on the eastern Tibetan Plateau in Sichuan, China (31°35′N, 102°35′E, and 3150 m a.s.l.). One site is a spruce-dominated natural forest (ca. 200 years old) and the other is a dragon spruce plantation (ca. 75 years old). The understorey of the natural forest is dominated by *Acer mono, Betula albosinensis* and *Lonicera* spp. Less vegetation is present in the spruce plantation, and *Festuca ovina, Deyeuxia rarundinacea,* and *Carex capilliformis* are the most common species growing under the plantation canopy. The mean annual precipitation and temperature are

800 mm and 8.9 °C, respectively. The growing season generally extends from late April to late October. According to the IUSS Working Group (2007), the acidic soils (pH 5.96 for the natural forest; pH 6.60 for the spruce plantation) are dark burozem and classified as Cambic Umbrisols.

2.2. Soil particle characterization

Three plots (10 m × 10 m) separated by more than 50 m were randomly delineated at each forest site. The sampling points were > 5 m apart, and the bulk soil samples (0–15 cm depth) were collected using a small trowel. Samples from three points in each plot were thoroughly mixed to obtain one composite sample and were immediately delivered to the laboratory (with ice bags). Each composite sample was passed through a 2 mm mesh sieve to remove organic plant materials and rocks. The basic soil properties (size 0–2 mm) in the organic horizon (0–15 cm) at the two sites are as follows: high clay (9.92 ± 1.83 %) and NH_4^+-N (22.47 ± 0.94 mg kg^{-1}) contents for natural forest; low clay (6.27 ± 1.54 %) and NH_4^+-N (15.19 ± 1.90 mg kg^{-1}) contents for spruce plantation. Fresh soils were dried naturally and separated into the following particle sizes: (i) clay (<2 μm), (ii) silt (2–53 μm), (iii) fine sand (53–250 μm), (iv) coarse sand (250–2000 μm) (Christensen, 1988) and (v) 0–2000 μm. The mass proportions of soil fractions (0–2000 μm) are as follows: clay 9.92 ± 1.83 %, silt 36.32 ± 4.0 % and sand 53.76 ± 5.8 % for the natural forest; clay 6.27 ± 1.54 %, silt 32.92 ± 2.5 % and sand 60.81 ± 4.09 % for the spruce plantation. The soil samples were steam pasteurized at 80 °C for 2 h every-two days. The great advantage of steam pasteurization was to reduce side effects on soil physico-chemical properties (Endlweber and Scheu, 2006).

Soil pH was determined at a solid-to-water ratio of 1:2.5 at room temperature using a pH meter (FE28, Mettler-Toledo, Switzerland). The concentrations of NO_3^--N and NH_4^+-N were obtained by the phenol disulfonic acid method and indophenol blue colorimetric method (Dorich and Nelson, 1983), respectively. The contents of TN and total organic carbon (TOC) in the soil were determined by an element analyser (Multi-N/C 2100, Analytik, Germany). The cation exchange capacity, specific surface area and mineral composition of the soil particles were analysed by $NH_4C_2H_3O_2$ displacement (Fagbenro and Agboola, 1999), the Brunauer-Emmett-Teller (BET) N_2 sorption method (Autosorb-1, Quantachrome, USA) and X-ray diffraction (D8 Advance, Bruker, Germany) (Cai et al., 2006), respectively. The zeta potentials of the soil particles were measured by a zeta potential analyser (Zetasizer Nano 3600, Malvern, UK) after they had passed through a 100-mesh sieve. The water contact angle was measured on the soil surfaces using an optical contact angle meter (DSA25, Kruss, Germany). The basic soil properties in both forests are shown in Table 1.

2.3. Quantitative real-time PCR (qPCR)

The abundance of archaeal and bacterial ammonia monooxygenase (*amoA)* genes was quantified by qPCR on a CFX96 Optical Real-Time Detection System (Bio-Rad Laboratories, Hercules, USA). PCR primers for amplifying archaeal and bacterial *amoA* genes were Arch-amoAF (STAATGGTCTGGCTTAGACG)/Arch-amoAR (GCGGCCATCCATCTGTATGT) (Francis et al., 2005) and amoA1F (GGGGTTTCTACTGGTGGT)/amoA2R (CCCCTCKGSAAAGCCTTCTTC) (Rotthauwe et al., 1998), respectively. Standard curves for each qPCR assay were obtained from one typical clone of the target gene sequence in a plasmid and diluted over a range of 10^1 to 10^9. The reaction mixtures (20 μl) contained 10 μl of SYBR Premix Ex Taq (Takapa, Dalian, China), 1.6 μl of DNA template (1–10 ng), 0.4 μl of each primer (10 mM) and 7.6 μl sterilized water. All samples were analysed in triplicate. Thermocycling conditions were performed at 95 °C for 5 min, followed by 40 cycles at 95 °C for 15 s, 60 °C for 30 s and a plate read after incubation at 78 °C for 10 s. Amplification efficiency was 86.3–94.0 % with R^2 values > 0.998. Amplification specificity was analyzed by melting curve analysis, which always results in a single peak.

2.4. Culture conditions

N. europaea (ATCC 19718) was cultivated in a constant-temperature shaking incubator (200 rpm) in the dark at 28 °C. Briefly, the cultivation medium recipe (L^{-1}) (1320 mg $(NH_4)_2SO_4$, 197 mg $MgSO_4{\cdot}7H_2O$, 14.7 mg $CaCl_2{\cdot}2H_2O$, 87.1 mg K_2HPO_4, 2553 mg $C_9H_{20}N_2O_4S$, 0.88 mg $C_{10}H_{12}FeN_2N_2NaO_8$, 0.01 mg $Na_2MoO_4{\cdot}2H_2O$, $MnCl_2{\cdot}4H_2O$, 0.01 mg $ZnSO_4{\cdot}7H_2O$, 0.0004 mg $CoCl_2{\cdot}6H_2O$ and 0.25 mg $CuSO_4{\cdot}5H_2O$) was the same as reported previously (Yu and Chandran, 2010) and the pH (7.5 ± 0.1) in the reactor was maintained via the addition of $NaHCO_3$ solution (40 g/L) until the late logarithmic phase (Morrow et al., 2005).The

Table 1
Measured properties of *N. europaea* and soil samples.

Bacteria/Soil particles	ZP (mV)	CEC (cmol kg^{-1})	WCA (°)	SSA (m^2/g)	C (%)	H (%)	K (%)	Q (%)	A (%)	NH_4^+-N (mg kg^{-1})	NO_3^--N (mg kg^{-1})	TOC (g kg^{-1})	TN (g kg^{-1})
N. *europaea*	−11.10 ± 0.87	–	–	–	–	–	–	–	–	–	–	–	–
NF-0–2 mm soil particle	−18.07 ± 0.36	26.25 ± 0.05	64.82 ± 5.55	34.36	19.43	4.64	5.86	54.98	15.09	22.47 ± 0.94	2.89 ± 0.25	59.11 ± 2.22	4.34 ± 0.07
NF-Clay	−12.90 ± 0.17	45.56 ± 0.06	15.81 ± 2.58	85.96	28.34	54.69	16.00	0.97	–	61.66 ± 2.28	2.78 ± 0.15	66.70 ± 0.34	6.22 ± 0.14
NF-Silt	−16.60 ± 1.06	19.70 ± 0.05	36.91 ± 2.43	8.10	13.64	3.85	3.04	63.20	16.28	19.02 ± 0.69	3.00 ± 0.11	35.59 ± 0.83	2.60 ± 0.06
NF-Fine sand	−16.97 ± 0.81	13.90 ± 0.04	49.07 ± 3.74	4.78	15.41	4.97	4.71	64.64	10.27	36.34 ± 0.90	4.89 ± 0.31	59.46 ± 3.73	3.69 ± 0.12
NF-Coarse sand	−19.87 ± 1.54	3.05 ± 0.04	72.51 ± 7.12	3.01	11.88	8.22	5.57	66.33	8.00	24.67 ± 0.94	1.91 ± 0.24	75.70 ± 4.20	4.47 ± 0.19
SP-0–2 mm soil particle	−19.10 ± 0.48	23.95 ± 0.07	73.66 ± 6.54	27.74	3.95	9.15	8.80	64.49	13.62	15.19 ± 1.90	2.17 ± 0.14	31.44 ± 0.97	2.88 ± 0.12
SP-Clay	−13.17 ± 0.78	41.40 ± 0.06	16.56 ± 1.84	77.93	9.19	75.39	14.51	0.91	–	60.23 ± 1.77	3.92 ± 0.23	57.07 ± 0.08	6.87 ± 0.12
SP-Silt	−17.04 ± 1.96	18.87 ± 0.04	33.64 ± 2.87	5.12	3.04	5.31	7.60	68.76	15.28	15.15 ± 0.82	2.52 ± 0.13	25.66 ± 0.42	2.31 ± 0.07
SP-Fine sand	−18.30 ± 0.96	11.6 ± 0.03	51.85 ± 3.41	3.84	3.02	10.74	9.68	62.73	13.82	39.90 ± 3.49	1.82 ± 0.16	91.66 ± 0.40	5.36 ± 0.20
SP-Coarse sand	−19.60 ± 0.80	2.25 ± 0.07	101.42 ± 5.66	2.85	6.95	21.89	15.07	48.55	7.54	26.25 ± 0.61	3.43 ± 0.06	35.56 ± 0.58	3.16 ± 0.17

ZP, zeta potential; CEC, cation exchange capacity; WCA, water contact angle; SSA, specific surface area; C, chlorite; H, hydromica; K, kaolinite; Q, quartz; A, albite; TOC, total organic carbon; TN, total nitrogen. Forest sites: NF, natural forest; SP, spruce plantation.

bacteria were harvested and centrifuged at 5500×*g* for 15 min. The pellet was washed twice with sterile phosphate buffered saline (PBS, pH 7.0) to remove all traces of growth medium. Finally, the cells were resuspended in PBS for subsequent use. The electrokinetic properties were measured by a zeta potential analyser (Zetasizer Nano 3600, Malvern, UK).

2.5. Batch adsorption experiments

2.5.1. Adsorption of NH_4^+-N on soils

NH_4^+-N adsorption isotherms were obtained by reacting 0–86.96 mg/L $(NH_4)_2SO_4$ with 100 mg steam-pasteurized soil particles at pH 7.0 in 30 mL PBS solution. These mixtures were shaken at 28 °C and 200 rpm for 24 h in the dark, and then the suspension was filtered through a 0.45-μm membrane syringe filter. The concentration of NH_4^+-N in the supernatant was determined by the Nesslerization colorimetric method (Jin and Tu, 1990). The concentration of NH_4^+-N adsorbed to soil particles was calculated from the amount of NH_4^+-N added and the remaining NH_4^+-N in the supernatant.

2.5.2. Adsorption of *N. europaea* on soils

N. europaea was cultured, collected and resuspended. Subsequently, batch adsorption experiments were conducted by mixing 100 mg steam-pasteurized soil particles with 30 mL PBS containing 0–15 × 10^{11} *N. europaea* cells. The mixtures were incubated at 28 °C for 1 h in the dark (sufficient for the reaction to reach a plateau) under shaking at 200 rpm. The growth and metabolism of *N. europaea* could be assumed to be negligible during the 1-h sorption process. The unadhered bacteria were separated from those adhered to soil particles by injecting 5 mL of sucrose solution (60 wt%) (Rong et al., 2008). Sucrose can create a density gradient in sorption systems. The suspension was centrifuged at 3500×*g* for 20 min, and the soil particle-cell aggregates sank to the bottom of the tubes (Rong et al., 2008). Preliminary experiments indicated that the sucrose solution had no significant effects on determining the number of *N. europaea*. According to a previously described method, the number of unadhered bacterial cells in the supernatant was determined by a UV–visible spectrophotometer (UV-1800, Shanghai Mapada, China) at a wavelength of 600 nm (Bradford, 1976; Jiang et al., 2007). The content of *N. europaea* protein was used to represent the abundance of bacteria. The abundance of *N. europaea* adsorbed to soil particles was calculated by the difference between the amount of added *N. europaea* and that remaining in the supernatant.

2.6. Oxidation kinetics of NH_4^+-N

A 50 mL wide-mouth glass flask that contained 5 mL of PBS were spiked with 100 mg steam-pasteurized soil particles and then dispersed by ultrasonication. *N. europaea* (7.5 × 10^{11} cells) was introduced into the systems. A known amount of $(NH_4)_2SO_4$ stock solution prepared in PBS was then added to the flasks to a final volume of 30 mL to obtain an initial N concentration of 43.48 mg/L (Fig. S1). The flasks were covered by sealing film with air-permeable holes to exclude external bacteria and impurities, then incubated in the dark at 28 °C and 200 rpm to ensure the oxygen saturation and to maintain the activity of bacteria as well as to encourage the interactions between NH_4^+-N, bacteria and soil particles. Each experiment set was performed in triplicate with a set of controls. The control experiments were conducted without bacteria. At regular time intervals, samples were removed, 0.5 % $HgCl_2$ was added to inhibit microbial activity, and the samples were filtered using a 0.45 μm membrane syringe filter. The NH_4^+-N concentrations in the filtrates were measured by the Nesslerization colorimetric method (Jin and Tu, 1990). Each flask, $(NH_4)_2SO_4$ and PBS solution were sterilized by autoclaving before the experiment. A solution without soil particles was used to calculated the initial concentration of NH_4^+-N.

2.7. Semipermeable membrane experiment

To explore the influence of bacterial adhesion in oxidation, a semipermeable membrane experiment was performed using a dialysis bag (MWCO, 8000–14,000). NH_4^+-N and PBS can freely pass across the dialysis bag, while bacteria and soil particles cannot (Fig. S1). Inside the dialysis bag, 100 mg steam-pasteurized soil particles were added. Outside the dialysis bag, bacterial suspension (2.5 × 10^{10} cells mL^{-1}), NH_4^+-N (43.48 mg/L), and PBS solution were placed in different flasks to obtain a final volume of 30 mL. Oxidation experiments in the presence of dialysis bags were conducted similar to those described in Section 2.6.

2.8. Micro-calorimetry experiments

The metabolic power-time curve of *N. europaea* in the absence or presence of soil particles was assessed by a TAM III thermal activity monitor (Thermometric AB, Jarfalla, Sweden). Before the experiment, 4 mL stainless steel ampoules were sterilized at 121 °C for 30 min. Twenty μL of *N. europaea* suspension (logarithmic anaphase) was inoculated into each ampoule containing 2 mL culture medium with or without 50 mg steam-pasteurized soil particles. A pure soil particle system (only soil particles without bacteria) was used as a negative control. After gentle shaking for 1 min, the ampoules were lowered to a preheating position on the equipment for 15 min at 28 °C and then to the measuring positions. Once the baseline was stable, the instrument began acquiring data until the signal returned to baseline again (Rong et al., 2007).

Each power-time curve includes the following two measurements: peak time (PT) and peak height (PH), which are commonly obtained from a TAM assistant software kit (TA Instrument, USA) (Barros et al., 1999). The final heat data for all soil particles-NH_4^+ + *N. europaea* systems is obtained by subtracting negative control levels. Here, PT is the time at which the calorimetric signal reaches its maximum thermal power, and PH is the maximum heat output at PT. According to previous literature reports, the microbial growth rate constant (μ) evaluated by micro-calorimetry is based on the assumption that the heat released from catabolic activities in the vegetative stage is proportional to the rate of cell division (Zhang et al., 2006). Hence, μ was calculated by fitting a logarithmic growth model based on the power-time curve data in the logarithmic growth stage.

2.9. Statistical analysis

To obtain good reproducibility, all experiments were performed in triplicate. Statistical differences were analysed with Student's *t* test, and $P < 0.05$ was taken to demonstrate a significant level throughout the study. All analyses were conducted using SPSS 22.0 software.

3. Results

3.1. AOA and AOB amoA gene analysis

The abundance of AOA and AOB *amoA* genes in the two contrasting forests was quantified by qPCR. The average abundance of ammonia oxidizers (AOA and AOB) was higher in the natural forest (AOA: 5.52 × 10^6 copies g^{-1} dry weight soil; AOB: 1.64 × 10^6 copies g^{-1} dry weight soil) than in the plantation (AOA: 1.15 × 10^6 copies g^{-1} dry weight soil; AOB: 7.25 × 10^5 copies g^{-1} dry weight soil) in the organic soil horizons.

3.2. Characterization of soil particles and N. europaea

The basic properties of the soils and *N. europaea* are summarized in Table 1. Generally, a large characteristic diversity was found among the different soil samples, with many of the differences being statistically significant ($P < 0.05$). The zeta potential, cation exchange capacity, and specific surface area of the soils decreased with increasing soil size, while the highest water contact angle was observed in coarse sand. All of

the particles (soil particles and cells) were negatively charged. The zeta potentials of *N. europaea*, natural forest soil and spruce plantation soil (0–2 mm) were −11.10 ± 0.87 mV, −18.07 ± 0.36 mV and −19.10 ± 1.54 mV, respectively. The zeta potentials of soils were in the range of −12.90 mV to −19.87 mV and −13.17 mV to −19.60 mV at various particle sizes (clay-coarse sand) in the natural forest and spruce plantation, respectively. Furthermore, the specific surface area of the natural forest soil (34.36 m^2/g) was 1.24 times higher than that of the spruce plantation soil (27.74 m^2/g). The specific surface areas were largest in clays and were significantly higher than those of silts and sands ($P < 0.05$). According to the mineral composition (Table 1), in addition to clay, the soil particles were composed of chlorite, hydromica, kaolinite, quartz and albite, and the quartz content was relatively high. The predominant mineral of the clay fractions was hydromica, and there were certain amounts of chlorite, kaolinite and quartz. Regarding 0–2 mm soil particles, the NH_4^+-N, NO_3^--N, TN and TOC contents were higher in the natural forest than in the spruce plantation (Table 1). Notably, the highest concentrations of NH_4^+-N and TN were observed in the clay fraction across the two contrasting forests.

3.3. Quantification of the attachment of NH_4^+-N and *N. europaea* to soil particles

The isotherms for NH_4^+-N and *N. europaea* sorption on different soil samples are depicted in Fig. S2 and Fig. 1, respectively. To quantitatively interpret the results, we fitted these data with the Langmuir model (Langmuir, 1917): $X = X_m KC/(1 + KC)$, where X is the amount of NH_4^+-N or cells adhered per unit mass of soils, X_m is the maximum adsorption of NH_4^+-N or cells, K is a constant related to adsorption energy and C is the concentration of NH_4^+-N or cells in the solution at equilibrium. As presented in Table S1 and Table S2, the Langmuir equation adequately described the adhesion, with R^2 (coefficient of determination) ranging from 0.948 to 0.998. Regarding 0–2 mm soil particles, the X_m values of NH_4^+-N and *N. europaea* adhesion to natural forest soil (2.703 mg g^{-1}; 72.288 × 10^{11} cells g^{-1}) were greater than those for spruce plantation soil (2.501 mg g^{-1}; 40.348 × 10^{11} cells g^{-1}). Additionally, clays were more effective than silts and sands in binding NH_4^+-N and bacterial cells regardless of forest site. For example, the amount of NH_4^+-N adsorbed on clay was 1.24–1.88 times greater than that on silts and sands in the natural forest, while it was 1.40–2.26 times greater in the spruce plantation (Table S1). Among the studied samples, the adsorption of cells on the surface of the natural forest soil increased by approximately 3.1-fold with increasing soil sizes from clay to coarse sand. In contrast, only a 1.9-fold increase was observed in the spruce plantation soil (Table S2).

3.4. Microbial oxidation of NH_4^+-N

To determine how much NH_4^+-N was present in the suspension and for how long it remained, the temporal development of NH_4^+-N in the batch incubations was assessed and is shown in Fig. 2. A first-order kinetics model was used to describe NH_4^+-N oxidation. The mathematical expression is $P = P_{max} \cdot (1 - e^{-kt})$, where P is the percentage of oxidation of NH_4^+-N, P_{max} is the maximal percent of oxidized substance, k is the first-order rate constant and t is the time (h) (Yang et al., 2010). Compared with the soil-free systems, the oxidation rate of NH_4^+-N was significantly decreased ($P < 0.05$) in the natural forest and spruce plantation treatments (Table 2). In the soil-free system, 90.3 % of NH_4^+-N was oxidised within 16 h, and 100 % oxidation was reached within 24 h. When 0–2 mm soil particles were present, NH_4^+-N oxidation dropped to 74.9 % and 80.3 % within 16 h and totally disappeared within 36 h in the natural forest and spruce plantation, respectively (Fig. 2a). The first-order rate constant for NH_4^+-N oxidation was 0.177 h^{-1} in the absence of soil and decreased to 0.084 h^{-1} and 0.109 h^{-1}, respectively, in the presence of 0–2 mm soil from the natural forest and the spruce plantation (Table 2). Additionally, the oxidation rates of NH_4^+-N by *N. europaea* followed the order coarse sand > fine sand > silt > clay (Table 2). For instance, with increasing in particle size in the spruce plantation system, the first-order rate constant of NH_4^+-N oxidation was 0.094 h^{-1} in the presence of clay and increased to 0.096 h^{-1}, 0.104 h^{-1}, and 0.121 h^{-1} in the presence of silt, fine sand and coarse sand, respectively.

3.5. Effect of semipermeable membranes on oxidation rate

To further verify whether the inhibition of NH_4^+-N oxidation by soil was caused by the association of bacterial cells with soil particles, a semipermeable membrane experiment was conducted. As shown in Table 2, we did not observe a significant difference in the first-order rate constants between the two forest sites ($P > 0.05$). The oxidation rates of NH_4^+-N in the semipermeable membrane systems were greater than those in the bacteria-adsorbed soil system but still lower than those in the soil-free system (Table 2). For example, in the natural forest soil (0–2 mm) semipermeable membrane system, NH_4^+-N oxidation reached 76.1 % within 12 h, which was significantly higher than that observed in the bacteria-adsorbed soil system (61.1 %) ($P < 0.05$).

3.6. Evaluation of metabolic activity of *N. europaea* in soil particles

To identify the metabolic activity of *N. europaea* as a function of time and exposure to different forest soil sites and size fractions, a heat flow analysis was conducted. The power-time curves of the logarithmic

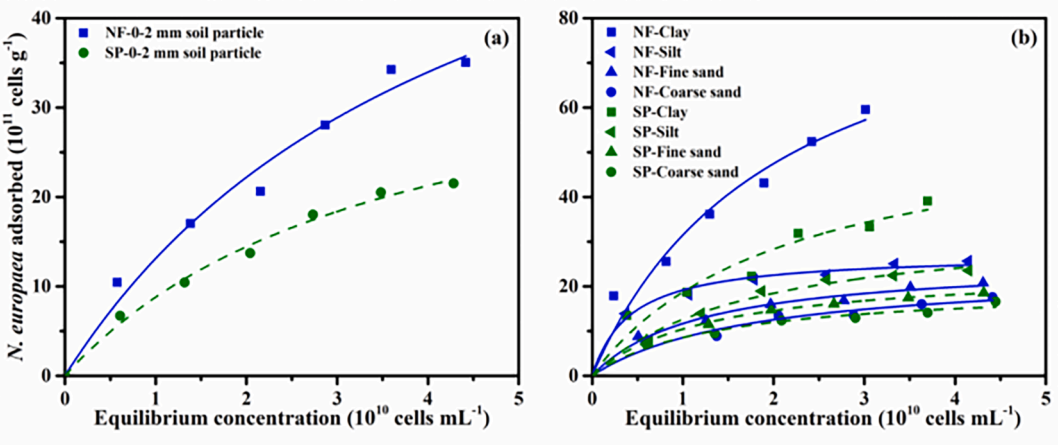

Fig. 1. Equilibrium sorption isotherms of *N. europaea* on forest soils (0–2 mm particles (a), particles with different sizes (clay-coarse sand) (b)). Experiments were carried out at pH 7.0 (28 °C) in PBS solution. The solid lines and dashed lines represent the fitted curves of Langmuir model curves for natural forest and spruce plantation, respectively. NF, natural forest; SP, spruce plantation.

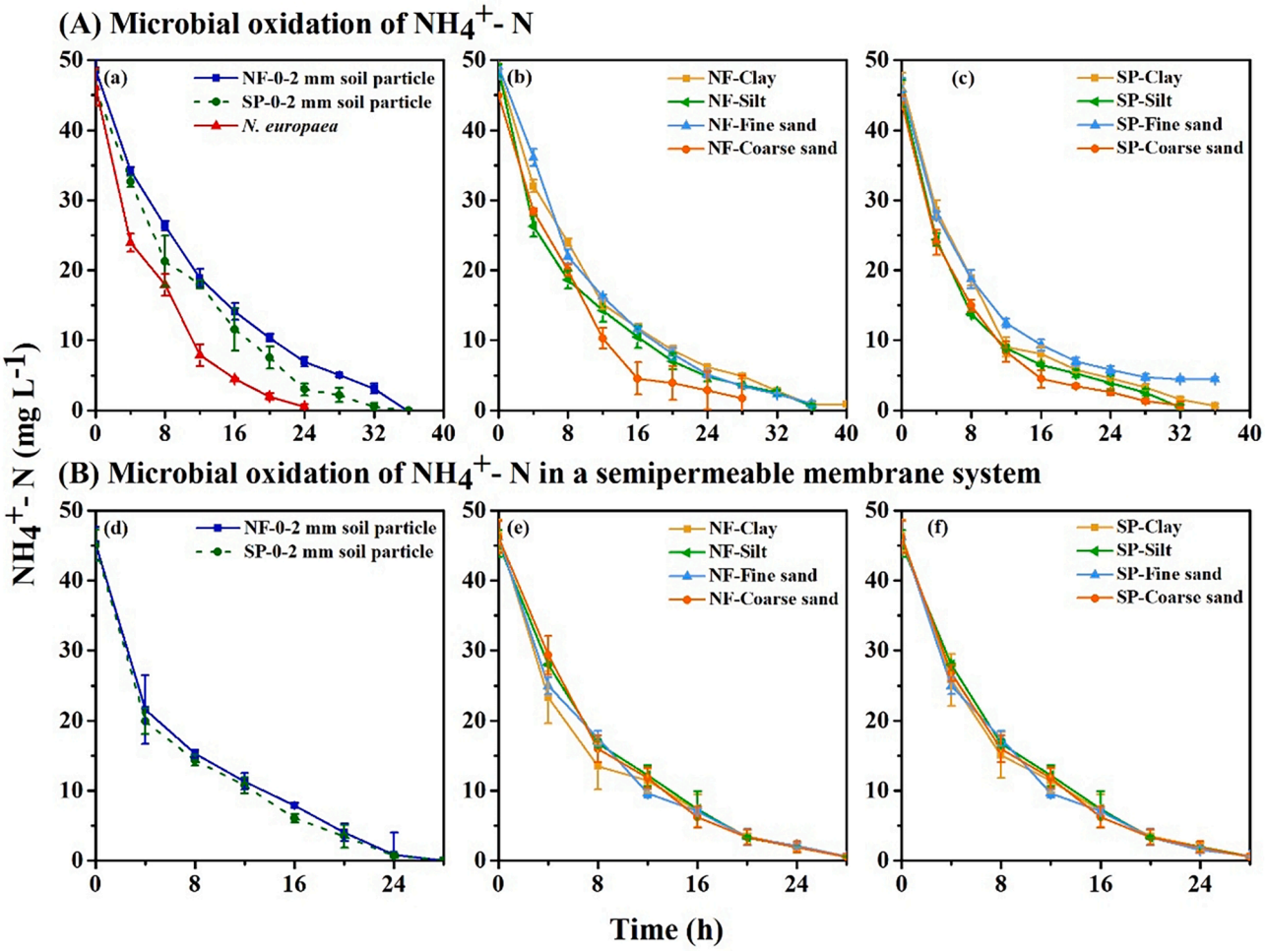

Fig. 2. Changes in NH_4^+-N concentration in the systems with (A) and without (B) the interfacial interactions between *N. europaea* and soil particles. Experiments were carried out at pH 7.0 (28 °C) in PBS solution. Red triangle indicates the positive control without soil particles; bule square and olive circle represents natural forest soils (0–2 mm) and spruce plantation soils (0–2 mm), respectively. Soil fractions were coded with yellow (clay), green (silt), light blue (fine sand) and orange (coarse sand) based on the particle sizes. Forest sites: NF (natural forest), SP (spruce plantation).

Table 2
First-order rate constants of NH_4^+-N oxidation by *N. europaea* at pH 7.0 (28 °C) in PBS solution.

Bacteria/soil particles	With interfacial interactions		Without interfacial interactions	
	k (h^{-1})	R^2	k (h^{-1})	R^2
Free *N. europaea*	–	–	0.177	0.971
NF-0–2 mm soil particle	0.084	0.995	0.145	0.942
NF-Clay	0.084	0.994	0.141	0.983
NF-Silt	0.088	0.994	0.145	0.971
NF-Fine sand	0.095	0.998	0.153	0.971
NF-Coarse sand	0.110	0.950	0.154	0.974
SP-0–2 mm soil particle	0.109	0.969	0.147	0.900
SP-Clay	0.094	0.971	0.144	0.970
SP-Silt	0.096	0.972	0.145	0.972
SP-Fine sand	0.104	0.991	0.145	0.983
SP-Coarse sand	0.121	0.985	0.147	0.974

k, first-order rate constant (h^{-1}); R^2, correlation coefficient. Forest sites: NF, natural forest; SP, spruce plantation.

growth of *N. europaea* in medium obey the thermodynamic equation $P_t = P_0 \exp(\mu t)$, where μ is the growth rate constant (min^{-1}) and P_t and P_0 represent the output power at time t and 0, respectively (μW) (Zhang et al., 2006). As depicted in the example thermogram (Fig. 3), the highest μ value was observed under the soil-free treatment, and the values decreased in the soil-containing systems (Table 3). Regarding 0–2 mm soil particles, bacterial metabolism exhibited a larger P_{max} under the spruce plantation treatment (6.971 μW) than under the natural forest treatment (6.421 μW). Furthermore, the value of μ increased with increasing soil particle size, varying from 0.0051 min^{-1} to 0.0094 min^{-1} in the natural forest treatment and 0.0058 min^{-1} to 0.0120 min^{-1} in the spruce plantation treatment (Table 3).

4. Discussion

The present data showed that ammonia oxidation was controlled by the interfacial interactions between soil particles and bacteria, with natural forest soil particles exhibiting more bacterial adhesion, less NH_4^+-N oxidation and weaker bacterial metabolic activity. Additionally, soil particles of different sizes with varied physico-chemical properties were found to largely influence interfacial interactions and NH_4^+-N content. The results from this study highlighted the importance of interfacial interactions in regulating NH_4^+-N availability in forest ecosystems, which can be helpful to predict AOB fate and activity in different forest soils.

Sorption is a critical process controlling bacterial mobility and the fate and bioavailability of nutrients in the environment (Tao et al., 2020). A growing body of evidence suggests that adsorption capacities are closely related to the surface physico-chemical properties of bacteria and soil particles (Haznedaroglu et al., 2008; Zhao et al., 2012; Cai et al.,

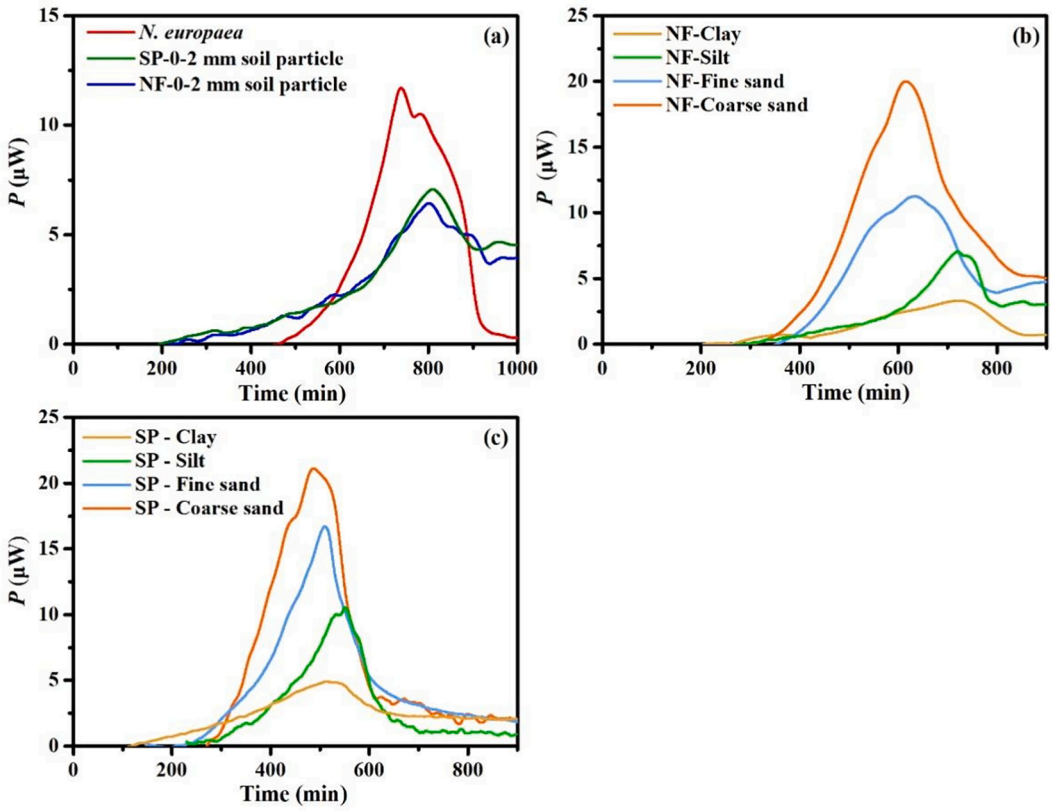

Fig. 3. Power-time curves for the growth of *N. europaea* influenced by soils (0–2 mm particles (a), particles with different sizes (clay-coarse sand) from natural forest (b) and spruce plantation (c)) at pH 7.5 (28 °C) in culture medium. NF, natural forest; SP, spruce plantation.

Table 3
Thermokinetic parameters for metabolic activities of free and bound *N. europaea* by soil particles at pH 7.5 (28 °C) in culture medium.

Systems	PH (μW)	PT (min)	μ (min^{-1})	R^2
Free *N. europaea*	11.701	738.232	0.0122	0.927
N. europaea + NF-0–2 mm soil particle	6.421	800.252	0.0058	0.978
N. europaea + NF-Clay	3.318	723.416	0.0051	0.962
N. europaea + NF-Silt	7.050	719.056	0.0084	0.948
N. europaea + NF-Fine sand	11.259	633.586	0.0087	0.903
N. europaea + NF-Coarse sand	19.990	614.280	0.0094	0.965
N. europaea + SP-0–2 mm soil particle	6.971	761.182	0.0060	0.986
N. europaea + SP-Clay	4.896	513.863	0.0058	0.972
N. europaea + SP-Silt	10.537	550.964	0.0094	0.985
N. europaea + SP-Fine sand	16.704	509.461	0.0100	0.983
N. europaea + SP-Coarse sand	21.102	485.849	0.0120	0.900

PH, peak heat, the maximum heat amplitude of the power-time curve; PT, peak time, when the calorimetric signal reaches the maximum; μ, growth rate constant of *N. europaea* in the logarithmic phase; R^2, correlation coefficient. Forest sites: NF, natural forest; SP, spruce plantation.

2018). It should be noted that natural forest soil had a higher clay content and adsorbed more bacteria than spruce plantation soil. The bacterial adsorption capacities were greater in clay particles than in silt and sand particles (Fig. 1b and Table S2), and were positively correlated with the parameters of zeta potential, cation exchange capacity and specific surface area. The smallest particle size fraction, clay, is composed principally of clay minerals, and the larger fractions (silt and sand) are composed mainly of primary minerals at different stages of weathering (Miao et al., 2016; Schulte et al., 2016). The soil clay fraction is considered the most active colloid that drives bacterial colonization (Uroz et al., 2015). Due to its high cation exchange capacity and specific surface area, clay provides more available surface sites or adsorbable nutrients on which bacteria can attach (Zhao et al., 2015; Cai et al., 2018). As indicated by the zeta potential values, the net surface charge of *N. europaea* and soil particles were all negative, yielding electrostatic repulsive forces (Kirby and Hasselbrink, 2004). More negative charges (absolute zeta potential value) result in stronger repulsive interactions. The surface charge of coarse sand was more negative than clay, which produced larger repulsive forces between *N. europaea* and coarse sand. By contrast, small net charges on clay enable bacteria access to the clay surface due to the relatively weak electrostatic repulsive forces between bacteria and clay. However, the contact angle of the soils was negatively correlated with X_m, which suggested that hydrophobic effects may also control the adsorption capacity. Smaller soil particles generally produced independent compartments for bacteria (Postma and Veen, 1990; Zhang et al., 2015), resulting in an increase in bacterial biomass in clay fractions compared with that of larger fractions. Precisely, it reflects our first hypothesis that bacterial adsorption on the soil surface could be explained by the combination of electrostatic forces and hydrophobic effects, which subsequently lead to divergent interfacial interactions between bacteria and soil.

In comparison with the soil-free treatment, the presence of soil retarded the oxidation rate of NH_4^+-N (Fig. 2 and Table 2). To maintain microbial growth, bacteria preferentially utilize free NH_4^+-N (Bollmann et al., 2002). It is reasonable to expect that the ammonia oxidation process would be inhibited by the presence of interfacial interactions between bacteria/NH_4^+-N and soils. Regarding 0–2 mm soil particles, the NH_4^+-N oxidation rate was higher in the spruce plantation than in the natural forest (Fig. 2a and Table 2), which provided an explanation for the previous report that the natural forest had greater soil NH_4^+-N availability than the spruce plantation (Zhang et al., 2018). Additionally, the oxidation rates in soil particles followed the order coarse sand

> fine sand > silt > clay, regardless of forest site (Fig. 2b, 2c and Table 2), whereas bacterial adsorption on soil particles displayed the opposite trend. In this study, more bacterial cells (68.4–73.3 %) and NH_4^+-N (58.7–65.2 %) were planktonic in the sand suspension. Under these conditions, a higher content of free NH_4^+-N would be consumed more quickly by the planktonic bacteria, while sorbed NH_4^+-N must be desorbed and then oxidised (Bouchez et al., 1995; Zhu et al., 2016). Furthermore, the semipermeable membrane experiment further suggested that the oxidation of NH_4^+-N increased when bacterial cells were not in contact with the soil surface, but still lower than soil-free treatment (Table 2). Although attached bacterial cells can utilize soil-sorbed NH_4^+-N, the tiny bacterial cells were encased in a dense matrix of extracellular polymeric substances and soil particles that form an aggregate to limit the diffusion of NH_4^+-N from the aqueous phase towards bacterial cells (Alimova et al., 2006; Mueller, 2015; Kleber et al., 2021), thus slowing down the rates of oxidation. In addition, no competitive adsorption between bacteria and NH_4^+-N. Another reasonable explanation for these findings is that an insufficient oxygen supply might negatively affect energy conversion and associated metabolisms, which resulted in lower bacterial activity (Schramm et al., 1996; Wu et al., 2018). In our study, bacteria cells tended to adsorb on clay and established a rather compact colonial structure, and the availability of oxygen for bacteria was lower (Yu and Chandran, 2010). Meanwhile, this strong association may deform cells, and ultimately cause the death of cells (Yu et al., 2015; Qu et al., 2019). Taken together, the ammonia oxidation rate was limited by the presence of interfacial interactions among soil particles (especially for clay) and bacterial cells, which could subsequently increase NH_4^+-N availability in forest soils.

The heat evolution from the metabolism of microbes is a reliable index of microbial activity and can be used to monitor bacterial activity throughout the oxidation process (Braissant et al., 2015). Under our experimental conditions, NH_4^+-N was the sole N source for bacterial metabolism. The differences in the heat signal between treatments can be attributed directly to the variations in *N. europaea* metabolic activities and NH_4^+-N oxidation levels. The highest metabolic activity was observed in the system without soil particles (Fig. 3 and Table 3), which suggested that soil particles could inhibit the metabolic activity of *N. europaea* via interfacial interactions. Regarding 0–2 mm soil particles, the metabolic activity of bacteria in the presence of spruce plantation soil was slightly higher than that in the presence of natural forest soil (Fig. 3a and Table 3). Additionally, bacterial metabolic activity was stimulated by the presence of sand and inhibited by clay (Fig. 3b, 3c and Table 3). Statistical analysis further showed that the bacterial metabolic activity was positively and linearly correlated with the NH_4^+-N oxidation rate ($R^2 = 0.68$; $P < 0.05$). The decreased activity of *N. europaea* under the natural forest treatment might also result from lower NH_4^+-N in the aqueous phase, since clay particles in natural forest soil effectively absorbed most of the NH_4^+-N provided (Table S1). In contrast, solution NH_4^+-N was consumed more efficiently by the planktonic bacteria, resulting in the growth of degrading bacteria in the sand system (Table 3). Collectively, our results indicated that the sand fraction provided a preferable microenvironment that was more conducive to bacterial metabolic activity than the silt and clay fractions, which is consistent with our second hypothesis.

Here we purpose a framework to illustrate the interfacial interaction mechanisms to alleviate inorganic N deficiency in two coniferous sites. In the absence of soil particles, free bacteria exhibited the greatest metabolic activity and oxidation rate; this may be attributable to the sufficient nutrient and oxygen supply. Compared with silt and sand particles, clay particles showed the greatest adsorption affinity for bacteria and NH_4^+-N, lowered bacterial activity and reduced ammonium oxidation, which means interfacial interaction will alleviate *N*-limited with increased the clay content (Fig. 4). The natural forest soil with a larger clay content display a higher adsorption affinity for AOM, weaker AOM metabolic activity and lower NH_4^+-N oxidation rate, probably contributed to the higher inorganic N availability. In contrast, the spruce plantation soil with greater sand content showed lower NH_4^+-N inorganic N availability due to its lower bacterial adsorption capacity, greater AOM metabolic activity and higher NH_4^+-N oxidation rate. Taken together, our study confirms that interfacial interactions alleviate inorganic N deficiency in alpine coniferous forest, and underline the importance of clay fractions in regulating bacteria metabolism activity.

Nevertheless, the extrapolation of these results should be considered with caution, given that the modeling methods were based on several

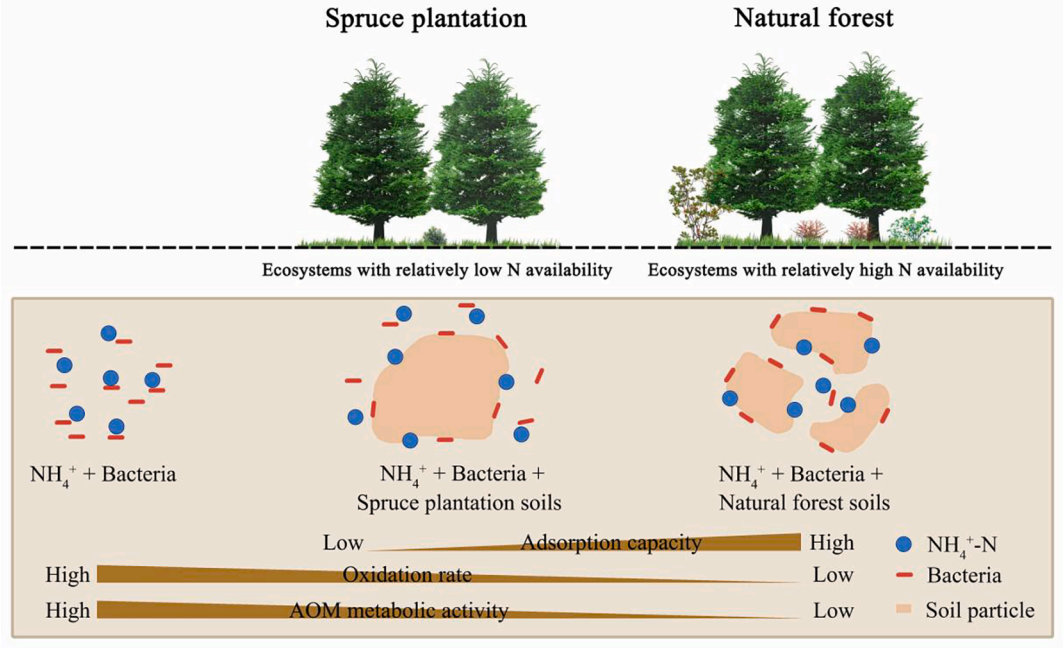

Fig. 4. Conceptual model illustrating the variation in the interfacial interaction effect on inorganic N availability in soil particles from the spruce plantation and natural forest. The blue dots and red and orange lines represent NH_4^+-N and bacteria and soil particles, respectively. The sizes of the arrows indicate the relative intensities of adsorption capacity, oxidation rate and AOM metabolic activities.

assumptions (Langmuir, 1917; Menert et al., 2001; Batstone et al., 2002). Currently, Langmuir, first-order kinetic and thermodynamic equation are widely used models to describe adsorption equilibrium, ammonia oxidation and bacterial metabolic activity, respectively (Ajeng et al., 2022; Lafratta et al., 2021; Morozova et al., 2020). In addition, measurements were made over limited two forest sites belonging to subalpine coniferous forest ecosystem and much work is needed to investigating the role of interfacial interactions effects on soil inorganic N availability in different forest types and ecosystems. Accordingly, although our study could not accurately exclude the impacts of modeling methods and forest sites, our results provide a new insight for understanding the role of interfacial interactions in controlling ammonia oxidation progresses in subalpine forest soils. Further research should focus on the development of novel techniques for obtaining more accurate estimates of the strength of interfacial interactions in ammonia oxidation patterns in different forest ecosystems.

5. Conclusions

Collectively, the above-discussed results provided the first robust evidence that interfacial interaction could directly regulate inorganic N availability in forest soils, which was associated with changes in the physicochemical features of soil particles with different sizes. Clay fractions have a protective strategy of soil inorganic N availability. The accumulation of substrate and bacteria on the clay surface greatly restricts the access of aerobic bacteria to the oxygen and limits the living space of particle-attached bacteria, resulting in decreased bacterial metabolic activity and NH_4^+-N oxidation rate. These findings highlight the need to incorporate interfacial interactions into the N cycling model to accurately predict AOM fate, soil N availability and their ecological feedbacks on forest ecosystem function, especially under future land use change. To expand the universality of interfacial interactions in this ternary system (N, AOM and soil particles), further experiments should focus on different AOM taxa and forest types.

Declaration of Competing Interest

The authors declare that they have no known competing financial interests or personal relationships that could have appeared to influence the work reported in this paper.

Data availability

No data was used for the research described in the article.

Acknowledgments

This work was supported by the projects of the National Natural Science Foundation of China (No. 31870607, 41930645 and 31971637), the Open Foundation of Ecological Security and Protection Key Laboratory of Sichuan Province of Mianyang Normal University (ESP1701), the Youth Innovation Promotion Association of the Chinese Academy of Sciences (2019363 and 2021371), the Sichuan Science and Technology Program (22ZDYF2279).

Appendix A. Supplementary data

Supplementary data to this article can be found online at https://doi.org/10.1016/j.geoderma.2022.116255.

References

Aftabtalab, A., Rinklebe, J., Shaheen, S.M., Niazi, N.K., Moreno-Jiménez, E., Schaller, J., Knorr, K.H., 2022. Review on the interactions of arsenic, iron (oxy)(hydr)oxides, and dissolved organic matter in soils, sediments, and groundwater in a ternary system. Chemosphere 286, 131790. https://doi.org/10.1016/j.chemosphere.2021.131790.

Ahmed, E., Holmström, S.J.M., 2015. Microbe-mineral interactions: The impact of surface attachment on mineral weathering and element selectivity by microorganisms. Chem. Geol. 403, 13–23. https://doi.org/10.1016/j.chemgeo.2015.03.009.

Ajeng, A.A., Abdullah, R., Ling, T.C., Ismail, S., 2022. Adhesion of *acillus salmalaya* and *Bacillus amyloliquefaciens* on oil palm kernel shell biochar: A physicochemical approach. J. Environ. Chem. Eng. 10, 107115 https://doi.org/10.1016/j.jece.2021.107115.

Alimova, A., Block, K., Rudolph, E., Katz, A., Steiner, J.C., Gottlieb, P., Alfano, R.R., 2006. Bacteria-clay interactions investigated by light scattering and phase contrast microscopy. Proc. SPIE. 60940E, 76–79. https://doi.org/10.1117/12.648042.

Asadishad, B., Ghoshal, S., Tufenkji, N., 2013. Short-term inactivation rates of selected gram-positive and gram-negative bacteria attached to metal oxide mineral surfaces: role of solution and surface chemistry. Environ. Sci. Technol. 47 (11), 5729–5737. https://doi.org/10.1021/es4003923.

Barros, N., Feijoó, S., Simoni, J.A., Prado, A.G.S., Barboza, F.D., Airoldi, C., 1999. Microcalorimetric study of some Amazonian soils. Thermochim Acta 328, 99–103. https://doi.org/10.1016/S0040-6031(98)00629-7.

Batstone, D.J., Keller, J., Angelidaki, I., Kalyuzhnyi, S.V., Pavlostathis, S.G., Rozzi, A., Sanders, W.T.M., Siegrist, H., Vavilin, V.A., 2002. Anaerobic Digestion Model, No. 1. IWA Publishing, London.

Biswas, B., Sarkar, B., Rusmin, R., Naidu, R., 2015. Bioremediation of PAHs and VOCs: Advances in clay mineral-microbial interaction. Environ. Int. 85, 168–181. https://doi.org/10.1016/j.envint.2015.09.017.

Bollmann, A., Bär-Gilissen, M.J., Laanbroek, H.J., 2002. Growth at low ammonium concentrations and starvation response as potential factors involved in niche differentiation among ammonia-oxidizing bacteria. Appl. Environ. Microbiol. 68 (10), 4751–4757. https://doi.org/10.1128/AEM.68.10.4751-4757.2002.

Bouchez, M., Blanchet, D., Vandecasteele, J.P., 1995. Substrate availability in phenanthrene biodegradation: transfer mechanism and influence on metabolism. Appl. Microbiol. Biot. 43 (5), 952–960. https://doi.org/10.1007/BF02431933.

Bradford, M.M., 1976. A rapid and sensitive method for the quantitation of microgram quantities of protein utilizing the principle of protein-dye binding. Anal. Biochem. 72 (1–2), 248–254. https://doi.org/10.1016/0003-2697(76)90527-3.

Braissant, O., Bachmann, A., Bonkat, G., 2015. Microcalorimetric assays for measuring cell growth and metabolic activity: Methodology and applications. Methods 76, 27–34. https://doi.org/10.1016/j.ymeth.2014.10.009.

Cai, P., Huang, Q.Y., Zhang, X.W., 2006. Interactions of DNA with clay minerals and soil colloidal particles and protection against degradation by DNase. Environ. Sci. Technol. 40 (9), 2971–2976. https://doi.org/10.1021/es0522985.

Cai, P., Liu, X., Ji, D., Yang, S., Walker, S.L., Wu, Y., Gao, C., Huang, Q., 2018. Impact of soil clay minerals on growth, biofilm formation, and virulence gene expression of *Escherichia coli* O157:H7. Environ. Pollut. 243, 953–960. https://doi.org/10.1016/j.envpol.2018.09.032.

Carnol, M., Kowalchuk, G.A., Boer, W.D., 2002. *Nitrosomonas europaea*-like bacteria detected as the dominant β-subclass *Proteobacteria* ammonia oxidisers in reference and limed acid forest soils. Soil Biol. Biochem. 34, 1047–1050. https://doi.org/10.1016/S0038-0717(02)00039-1.

Chen, H.S., Xu, J.L., Tan, W.F., Fang, L.C., 2019. Lead binding to wild metal-resistant bacteria analyzed by ITC and XAFS spectroscopy. Environ. Pollut. 250, 118–126. https://doi.org/10.1016/j.envpol.2019.03.123.

Christensen, B.T., 1988. Effects of animal manure and mineral fertilizer on the total carbon and nitrogen contents of soil size fractions. Biol. Fertil. Soils 5, 304–307. https://doi.org/10.1007/bf00262136.

Combarros, R.G., Collado, S., Díaz, M., 2016. Toxicity of graphene oxide on growth and metabolism of *Pseudomonas putida*. J. Hazard. Mater. 310, 246–252. https://doi.org/10.1016/j.jhazmat.2016.02.038.

Cuadros, J., 2017. Clay minerals interaction with microorganisms: a review. Clay Miner. 52 (2), 235–261. https://doi.org/10.1180/claymin.2017.052.2.05.

Dorich, R.A., Nelson, D.W., 1983. Direct colorimetric measurement of ammonium in potassium chloride extracts of soils. Soil Sci. Soc. Am. J. 47 (4), 833–836. https://doi.org/10.2136/sssaj1983.03615995004700040042x.

Elbourne, A., Chapman, J., Gelmi, A., Cozzolino, D., Crawford, R.J., Truong, V.K., 2019. Bacterial-nanostructure interactions: The role of cell elasticity and adhesion forces. J. Colloid Interface Sci. 546, 192–210. https://doi.org/10.1016/j.jcis.2019.03.050.

Endlweber, K., Scheu, S., 2006. Establishing arbuscular mycorrhiza-free soil: A comparison of six methods and their effects on nutrient mobilization. Appl. Soil Ecol. 34, 276–279. https://doi.org/10.1016/j.apsoil.2006.04.001.

Fagbenro, J.A., Agboola, A.A., 1999. Effect of aerial oxidation pretreatment on composition and effectiveness of a Nigerian lignite sample as soil organic matter amendment. Commun. Soil Sci. Plan. 30 (17–18), 2331–2344. https://doi.org/10.1080/00103629909370377.

Francis, C.A., Roberts, K.J., Beman, J.M., Santoro, A.E., Oakley, B.B., 2005. Ubiquity and diversity of ammonia-oxidizing archaea in water columns and sediments of the ocean. PANS 102, 14683–14688. https://doi.org/10.1073/pnas.0506625102.

Fraser, T.D., Lynch, D.H., Bent, E., Entz, M.H., Dunfield, K.E., 2015. Soil bacterial *phoD* gene abundance and expression in response to applied phosphorus and long-term management. Soil Biol. Biochem. 88, 137–147. https://doi.org/10.1016/j.soilbio.2015.04.014.

Gold, K., Slay, B., Knackstedt, M., Gaharwar, A.K., 2018. Antimicrobial activity of metal and metal-oxide based nanoparticles. Adv. Ther. 1, 1700033. https://doi.org/10.1002/adtp.201700033.

Gupta, N., Sen, R., 2017. Kinetic and equilibrium modelling of Cu (II) adsorption from aqueous solution by chemically modified Groundnut husk (Arachis hypogaea). J. Environ. Eng. 5, 4274–4281. https://doi.org/10.1016/j.jece.2017.07.048.

Han, S., Luo, X.S., Tan, S., Wang, J.F., Chen, W.L., Huang, Q.Y., 2020. Soil aggregates impact nitrifying microorganisms in a vertisol under diverse fertilization regimes. Eur. J. Soil Sci. 71, 536–547. https://doi.org/10.1111/ejss.12881.

Han, S., Delgado-Baquerizo, M., Luo, X.S., Liu, Y.R., Nostrand, J.D.V., Chen, W.L., Zhou, J.Z., Huang, Q.Y., 2021. Soil aggregate size-dependent relationships between microbial functional diversity and multifunctionality. Soil Biol. Biochem. 154, 108143. https://doi.org/10.1016/j.soilbio.2021.108143.

Haznedaroglu, B.Z., Bolster, C.H., Walker, S.L., 2008. The role of starvation on *Escherichia coli* adhesion and transport in saturated porous media. Water Res. 42, 1547–1554. https://doi.org/10.1016/j.watres.2007.10.042.

He, L., Rong, H.F., Li, M., Zhang, M.Y., Liu, S.R., Yang, M., Tong, M.P., 2021. Bacteria have different effects on the transport behaviors of positively and negatively charged microplastics in porous media. J. Hazard. Mater. 415, 125550. https://doi.org/10.1016/j.jhazmat.2021.125550.

Hong, Z.N., Yan, J., Lu, H.L., Jiang, J., Li, J.Y., Xu, R.K., 2021. Inhibition of phosphate sorptions on four soil colloids by two bacteria. Environ. Pollut. 290, 118001 https://doi.org/10.1016/j.envpol.2021.118001.

Jiang, D.H., Huang, Q.Y., Cai, P., Rong, X.M., Chen, W.L., 2007. Adsorption of *Pseudomonas putida* on clay minerals and iron oxide. Colloid Surface B. 54, 217–221. https://doi.org/10.1016/j.colsurfb.2006.10.030.

Jin, X., Tu, Q., 1990. The Standard Methods for Observation and Analysis in Lake Eutrophication. Chinese environment science press, Beijing.

Kirby, B.J., Hasselbrink E.F., Jr, 2004. Zeta potential of microfluidic substrates: 1. Theory, experimental techniques, and effects on separations. Electrophoresis 25, 187–202. https://doi.org/10.1002/elps.200305754.

Kleber, M., Bourg, I.C., Coward, E.K., Hansel, C.M., Myneni, S.C.B., Nunan, N., 2021. Dynamic interactions at the mineral–organic matter interface. Nat. Rev. Earth Environ. 2, 402–421. https://doi.org/10.1038/s43017-021-00162-y.

Lafratta, M., Thorpe, R.B., Ouki, S.K., Shana, A., Germain, E., Willcocks, M., Lee, J., 2021. Development and validation of a dynamic first order kinetics model of a periodically operated well-mixed vessel for anaerobic digestion. Chen. Eng. J. 426, 131732 https://doi.org/10.1016/j.cej.2021.131.

Langmuir, I., 1917. The constitution and fundamental properties of solids and liquids. II. Liquids. J. Am. Chem. Soc. 39, 1858–1906. https://doi.org/10.1016/s0016-0032(17)09038-x.

Li, T., He, Y.H., An, X.F., Li, C., Wu, Z.S., 2021. Elucidating adhesion behaviors and the interfacial interactions between plant probiotics and modified bentonite carriers. ACS Sustain. Chem. Eng. 9, 8125–8135. https://doi.org/10.1021/acssuschemeng.1c01166.

Li, H., Hollstein, M., Podder, A., Gupta, V., Barber, M., Goel, R., 2020. Cyanotoxin impact on microbial-mediated nitrogen transformations at the interface of sediment-water column in surface water bodies. Environ. Pollut. 266, 115283. https://doi.org/10.1016/j.envpol.2020.115283.

Liu, X., Gao, C.H., Ji, D.D., Walker, S.L., Huang, Q.Y., Cai, P., 2017. Survival of *Escherichia coli* O157:H7 in various soil particles: importance of the attached bacterial phenotype. Biol. Fertil. Soils 53, 209–219. https://doi.org/10.1007/s00374-016-1172-y.

Liu, L.Y., Tan, Z.X., Gong, H.B., Huang, Q.Y., 2018. Migration and transformation mechanisms of mutrient elements (N, P, K) within biochar in straw-biochar-soil-plant systems: a review. ACS Sustain. Chem. Eng. 7, 22–32. https://doi.org/10.1021/acssuschemeng.8b04253.

Lu, J.K., Luo, Y.N., Huang, J.L., Hou, B.Y., Wang, B., Qgino, K.J., Zhao, J., Si, H.Y., 2022. The effect of biochar on the migration theory of nutrient ions. Sci. Total Environ. 845, 157262 https://doi.org/10.1016/j.scitotenv.2022.157262.

Lyon, D.Y., Brunet, L., Hinkal, G.W., Wiesner, M.R., Alvarez, P.J.J., 2008. Antibacterial activity of fullerene water suspensions (nC_{60}) is not due to ROS-mediated damage. Nano Lett. 8 (5), 1539–1543. https://doi.org/10.1021/nl0726398.

Malham, S.K., Rajko-Nenow, P., Howlett, E., Tuson, K.E., Perkins, T.L., Pallett, D.W., Wang, H., Jago, C.F., Jones, D.L., McDonald, J.E., 2014. The interaction of human microbial pathogens, particulate material and nutrients in estuarine environments and their impacts on recreational and shellfish waters. Environ. Sci. Proc. Imp. 16, 2145–2155. https://doi.org/10.1039/c4em00031e.

Martinez, R.E., Konhauser, K.O., Paunova, N., Wu, W., Alessi, D.S., Kappler, A., 2016. Surface reactivity of the anaerobic phototrophic Fe(II)-oxidizing bacterium Rhodovulum iodosum: Implications for trace metal budgets in ancient oceans and banded iron formations. Chem. Geol. 442, 113–120. https://doi.org/10.1016/j.chemgeo.2016.09.004.

Menert, A., Liiders, M., Kurissoo, T., Vilu, R., 2001. Microcalorimetric monitoring of anaerobic digestion processes. J. Therm. Anal. Calorim. 64, 281–291. https://doi.org/10.1023/a:1011513819091.

Miao, W.L., Fan, Q.S., We, H.C., Zhang, X.Y., Ma, H.Z., 2016. Clay mineralogical and geochemical constraints on late Pleistocene weathering processes of the Qaidam Basin, northern Tibetan Plateau. J. Asian Earth Sci. 127, 267–280. https://doi.org/10.1016/j.jseaes.2016.06.013.

Mohamed, A., Yu, L., Fang, Y., Ashry, N., Riahi, Y., Uddin, I., Dai, K., Huang, Q.Y., 2020. Iron mineral-humic acid complex enhanced Cr(VI) reduction by *Shewanella oneidensis* MR-1. Chemosphere 247, 125902. https://doi.org/10.1016/j.chemosphere.2020.125902.

Morozova, K., Armani, M., Scampicchio, M., 2020. Isothermal calorimetry for monitoring of grape juice fermentation with yeasts immobilized on nylon-6 nanofibrous membranes. J. Therm. Anal. Calorim. 139, 375–382. https://doi.org/10.1007/s10973-019-08370-x.

Morrow, J.B., Stratton, R., Yang, H.Z.H., Smets, B.F., Grasso, D., 2005. Macro- and nanoscale observations of adhesive behavior for several *E. coli* strains (O157:H7 and environmental isolates) on mineral surfaces. Environ. Sci. Technol. 39, 6395–6404. https://doi.org/10.1021/es0500815.

Mueller, B., 2015. Experimental interactions between clay minerals and bacteria: A review. Pedosphere 25, 799–810. https://doi.org/10.1016/S1002-0160(15)30061-8.

Nell, R.M., Fein, J.B., 2017. Influence of sulfhydryl sites on metal binding by bacteria. Geochim. Cosmochim. Acc. 199, 210–221. https://doi.org/10.1016/j.gca.2016.11.039.

Plaimart, J., Acharya, K., Mrozik, W., Davenport, R.J., Vinitnantharat, S., Werner, D., 2021. Coconut husk biochar amendment enhances nutrient retention by suppressing nitrification in agricultural soil following anaerobic digestate application. Environ. Pollut. 268, 115684 https://doi.org/10.1016/j.envpol.2020.115684.

Postma, J., Veen, J.A.v., 1990. Habitable pore space and survival of *Rhizobium leguminosarum biovartrifolii* introduced into soil. Microb. Ecol. 19, 149–161. https://doi.org/10.1007/BF02012096.

Pronk, G.J., Heister, K., Vogel, C., Babin, D., Bachmann, J., Ding, G.C., Ditterich, F., Gerzabek, M.H., Giebler, J., Hemkemeyer, M., Kandeler, E., Mouvenchery, Y.K., Miltner, A., Poll, C., Schaumann, G.E., Smalla, K., Steinbach, A., Tanuwidjaja, I., Tebbe, C.C., Wick, L.Y., Woche, S.K., Totsche, K.U., Schloter, M., Kögel-Knabner, I., 2016. Interaction of minerals, organic matter, and microorganisms during biogeochemical interface formation as shown by a series of artificial soil experiments. Biol. Fertil. Soils 53 (1), 9–22. https://doi.org/10.1007/s00374-016-1161-1.

Putnis, A., 2014. Why mineral interfaces matter. Science 343, 1441–1442. https://doi.org/10.1126/science.1250884.

Putnis, C.V., Ruiz-Agudo, E., 2013. The mineral-water interface: where minerals react with the environment. Elements 9 (3), 177–182. https://doi.org/10.2113/gselements.9.3.177.

Qu, C.C., Qian, S.F., Chen, L., Guan, Y., Zheng, L., Liu, S.H., Chen, W.L., Cai, P., Huang, Q.Y., 2019. Size-dependent bacterial toxicity of hematite particles. Environ. Sci. Technol. 53, 8147–8156. https://doi.org/10.1021/acs.est.9b00856.

Rong, X.M., Huang, Q.Y., Chen, W.L., 2007. Microcalorimetric investigation on the metabolic activity of *Bacillus thuringiensis* as influenced by kaolinite, montmorillonite and goethite. Appl. Clay Sci. 38, 97–103. https://doi.org/10.1016/j.clay.2007.01.015.

Rong, X.M., Huang, Q.Y., He, X.M., Chen, H., Cai, P., Liang, W., 2008. Interaction of *Pseudomonas putida* with kaolinite and montmorillonite: A combination study by equilibrium adsorption, ITC, SEM and FTIR. Colloid Surface B. 64, 49–55. https://doi.org/10.1016/j.colsurfb.2008.01.008.

Rong, X.M., Zhao, G., Fein, J.B., Yu, Q., Huang, Q.Y., 2019. Role of interfacial reactions in biodegradation: A case study in a montmorillonite, *Pseudomonas* sp. Z1 and methyl parathion ternary system. J. Hazard. Mater. 365, 245–251. https://doi.org/10.1016/j.jhazmat.2018.11.019.

Rotthauwe, J.J., Witzel, K.P., Liesack, W., 1998. The ammonia monooxygenase structural gene *amoA* as a functional marker: molecular fine-scale analysis of natural ammonia-oxidizing populations. Appl. Environ. Microbiol. 63, 4704–4712. https://doi.org/10.1128/AEM.63.12.4704-4712.1997.

Schramm, A., Larsen, L.H., Revsbech, N.P., Ramsing, N.B., Amann, R., Schleifer, K.H., 1996. Structure and function of a nitrifying bioflm as determined by in situ hybridization and the use of microelectrodes. Appl. Environ. Microbiol. 62, 4641–4647. https://doi.org/10.1128/AEM.62.12.4641-4647.1996.

Schulte, P., Lehmkuhl, F., Steininger, F., Loibl, D., Lockot, G., Protze, J., Fischer, P., Stauch, G., 2016. Influence of HCl pretreatment and organo-mineral complexes on laser diffraction measurement of loess-paleosol-sequences. Catena 137, 392–405. https://doi.org/10.1016/j.catena.2015.10.015.

Small, P., Blankenhorn, D., Welty, D., Zinser, E., Slonczewski, J.L., 1994. Acid and base resistance in *Escherichia coli* and *Shigella flexneri*: role of rpoS and growth pH. J. Bacteriol. 176, 1729–1737. https://doi.org/10.1128/jb.176.6.1729-1737.1994.

Stone, W., Kroukamp, O., Korber, D.R., McKelvie, J., Wolfaardt, G.M., 2016. Microbes at surface-air interfaces: The metabolic harnessing of relative humidity, surface hygroscopicity, and oligotrophy for resilience. Front. Microbiol. 7, 1563. https://doi.org/10.3389/fmicb.2016.01563.

Tao, Y., Han, S.Y., Zhang, Q., Yang, Y., Shi, H.T., Akindolie, A.S., Jiao, Y.Q., Qu, J.H., Jiang, Z., Han, W., Zhang, Y., 2020. Application of biochar with functional microorganisms for enhanced atrazine removal and phosphorus utilization. J. Clean. Prod. 257, 120535 https://doi.org/10.1016/j.jclepro.2020.120535.

Uroz, S., Kelly, L.C., Turpault, M.P., Lepleux, C., Frey-Klett, P., 2015. The mineralosphere concept: mineralogical control of the distribution and function of mineral-associated bacterial communities. Trends Microbiol. 23, 751–762. https://doi.org/10.1016/j.tim.2015.10.004.

Wang, L.J., Putnis, C.V., 2020. Dissolution and precipitation dynamics at environmental mineral interfaces imaged by in situ atomic force microscopy. Acc. Chem. Res. 53, 1196–1205. https://doi.org/10.1021/acs.accounts.0c00128.

Wu, Y.C., Cai, P., Jing, X.X., Niu, X.K., Ji, D.D., Ashry, N.M., Gao, C.H., Huang, Q.Y., 2019. Soil biofilm formation enhances microbial community diversity and metabolic activity. Environ. Int. 132, 105116 https://doi.org/10.1016/j.envint.2019.105116.

Wu, J.K., Zhan, M.J., Chang, Y., Su, Q.X., Yu, R., 2018. Adaption and recovery of *Nitrosomonas europaea* to chronic TiO_2 nanoparticle exposure. Water Res. 147, 429–439. https://doi.org/10.1016/j.watres.2018.09.043.

Xia, X.H., Yang, Z.F., Zhang, X.Q., 2009. Effect of suspended-sediment concentration on nitrification in river water: importance of suspended sediment-water interface. Environ. Sci. Technol. 43, 3681–3687. https://doi.org/10.1021/es8036675.

Yang, Y., Shu, L., Wang, X., Xing, B., Tao, S., 2010. Effects of composition and domain arrangement of biopolymer components of soil organic matter on the bioavailability of phenanthrene. Environ. Sci. Technol. 44 (9), 3339–3344. https://doi.org/10.1021/es903586v.

Yu, R., Chandran, K., 2010. Strategies of *Nitrosomonas europaea* 19718 to counter low dissolved oxygen and high nitrite concentrations. BMC Microbiol. 10, 70. https://doi.org/10.1186/1471-2180-10-70.

Yu, R., Fang, X.H., Somasundaran, P., Chandran, K., 2015. Short-term effects of TiO2, CeO2, and ZnO nanoparticles on metabolic activities and gene expression of *Nitrosomonas europaea*. Chemosphere 128, 207–215. https://doi.org/10.1016/j.chemosphere.2015.02.002.

Zhang, Z.L., Li, N., Xiao, J., Zhao, C.Z., Zou, T.T., Li, D.D., Liu, Q., Yin, H.J., 2018. Changes in plant nitrogen acquisition strategies during the restoration of spruce plantations on the eastern Tibetan Plateau, China. Soil Biol. Biochem. 119, 50–58. https://doi.org/10.1016/j.soilbio.2018.01.002.

Zhang, Q., Liang, G.Q., Myrold, D.D., Zhou, W., 2017. Variable responses of ammonia oxidizers across soil particle-size fractions affect nitrification in a long-term fertilizer experiment. Soil Biol. Biochem. 105, 25–36. https://doi.org/10.1016/j.soilbio.2016.11.005.

Zhang, L.X., Liu, Y, Cia, L.H., Hu, Y.J., Yin, J., Hu, P.Z., 2006. Inhibitory study of some novel Schiff base derivatives on *Staphylococcus aureus* by microcalorimetry. Thermochim. Acta 440 (1), 51–56. https://doi.org/10.1016/j.tca.2005.10.012.

Zhang, Q., Zhou, W., Liang, G.Q., Sun, J.W., Wang, X.B., He, P., 2015. Distribution of soil nutrients, extracellular enzyme activities and microbial communities across particle-size fractions in a long-term fertilizer experiment. Appl. Soil Ecol. 94, 59–71. https://doi.org/10.1016/j.apsoil.2015.05.005.

Zhao, G., Li, E., Li, J.J., Xu, M.Y., Huang, Q.Y., Rong, X.M., 2018. Effects of interfaces of goethite and humic acid-goethite complex on microbial degradation of methyl parathion. Front. Microbiol. 9, 1748. https://doi.org/10.3389/fmicb.2018.01748.

Zhao, W.Q., Liu, X., Huang, Q.Y., Rong, X.M., Liang, W., Dai, K., Cai, P., 2012. Sorption of *Streptococcus suis* on various soil particles from an Alfisol and effects on pathogen metabolic activity. Eur. J. Soil Sci. 63, 558–564. https://doi.org/10.1111/j.1365-2389.2012.01469.x.

Zhao, W.Q., Liu, X., Huang, Q.Y., Cai, P., 2015. *Streptococcus suis* sorption on agricultural soils: Role of soil physico-chemical properties. Chemosphere 119, 52–58. https://doi.org/10.1016/j.chemosphere.2014.05.060.

Zhu, X.Y., Wang, K., Yan, H.C., Liu, C.C., Zhu, X.Y., Chen, B.L., 2022. Microfluidics as an emerging platform for exploring soil environmental processes: A critical review. Environ. Sci. Technol. 56, 711–731. https://doi.org/10.1021/acs.est.1c03899.

Zhu, B.T., Xia, X.H., Wu, S., Lu, X.X., Yin, X.N., 2016. Microbial bioavailability of 2,2',4,4'-Tetrabromodiphenyl ether (BDE-47) in natural sediments from major rivers of China. Chemosphere 153, 386–393. https://doi.org/10.1016/j.chemosphere.2016.03.050.

Zobell, C.E., 1943. The effect of solid surfaces upon bacterial activity. J. Bacteriol. 46 (1), 39–56. https://doi.org/10.1128/JB.46.1.39-56.1943.